Temperature-dependent viscous gravity currents with shear heating

Oleg V. Vasilyev[a)]
Mechanical and Aerospace Engineering, University of Missouri–Columbia, Columbia, Missouri 65211

Arkady A. Ten and David A. Yuen[b)]
Minnesota Supercomputing Institute and Department of Geology and Geophysics, University of Minnesota, Minneapolis, Minnesota 55415

(Received 24 August 2000; accepted 7 September 2001)

We have studied the effects of viscous dissipation on gravity current in the Stokes flow regime for both constant volume and constant flux boundary conditions. We have also examined the influence of temperature-dependent viscosity, as well as the relative importance of thermal and chemical buoyant forces. For the constant volume case a three-stage evolution was found. This aspect concerning the existence of the multiple stages is new and was not found previously. This three-stage behavior comes as a result of the interaction between the two quasi-isothermal regimes. The first regime corresponds to an early stage with a uniformly high temperature, whereas the third stage represents the final period, when most part of the current has cooled down to uniformly low temperature. This evolutionary process with three-stages is characteristic of a temperature-dependent viscous fluid and does not depend too much on viscous dissipation, which induces a longer transient period. In contrast to constant volume case, there is only one stage of development for the constant flux current. Although temperature-dependent viscosity influences the current dynamics, the rate of expansion follows a $t^{1/2}$ asymptote which is close to the prediction for a constant viscosity model with a constant flux condition. Viscous dissipation exerts definitely a stronger influence in the constant flux gravity currents as compared to the constant volume case, because of the faster velocities produced by the constant flux condition. [DOI: 10.1063/1.1416501]

I. INTRODUCTION

Gravity currents are commonly found in nature[1] and involve the horizontal spreading of fluid masses being driven by gravitational forces. In the low Reynolds number limit and with negligible surface tension, gravity currents are important for the manufacture of glass,[2–4] ice sheets,[5,6] lava-flows,[7,8] and mantle dynamics.[9–11]

From their narrow geometry, gravity currents can be classified as having boundary-layer flow character. Viscous heating has been found to be significant in the thermal boundary layers of high-Rayleigh number and infinite Prandtl number 3D convection in the mantle, where the Reynolds number is effectively zero, for both depth-dependent[12,13] and variable viscosity.[13–15] Viscous dissipation is concentrated in the vertical and the horizontal boundary layers as modeled in mantle convection,[16] where most of the shear deformation takes place, e.g., Refs. 17 and 18. In all of the previous research on gravity currents, the effects of viscous dissipation have been ignored: In experimental studies[19] because of scaling difficulties in the laboratory and also in analytical and numerical studies because of the high spatial resolution required in problems involving shear heating.[20]

In this work we will focus our attention on the effects of viscous dissipation upon gravity currents for two different types of boundary conditions, which deal with the conservation of mass.[10] Both constant and temperature-dependent viscosity will be considered for these types of boundary conditions.

II. MODEL

In this section we present the model equations for the coupled thermo-mechanical problem of gravity currents. This model is an extension of the one developed by Bercovici and Lin.[11] The proposed model includes the effects of viscous-heating, thermal buoyancy and temperature-dependent viscosity. Following the theories of axi-symmetric gravity currents,[10,11,21] we assume radial creeping flow of hot and/or light Boussinesq fluid cooling through two horizontal boundaries, at least one of which is deformable. The model setup of the flow is displayed in Fig. 1 and parameters relevant to the problem are described in Table I. Note that in this study we assume that the lower boundary of the current, $z=H$, is deformable, i.e., $H=H(r,t)$. However, the model can be easily applied to the case when both boundaries are deformable. In this case H represents the total thickness of the gravity current.

Following Bercovici[10] and Bercovici and Lin[11] we assume that the density of the gravity current is given by

a)Author to whom correspondence should be addressed. Telephone: (573) 882-3755; Fax: (573) 884-5090. Electronic mail: vasilyevo@missouri.edu
b)Electronic mail: davey@krissy.msi.umn.edu

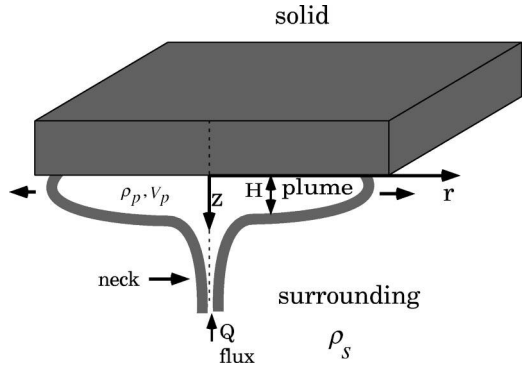

FIG. 1. Schematic diagram showing the axi-symmetric temperature-dependent gravity model. The coordinate system consists of the radial r and the depth z axis. A solid stratum is present at the top. The temperature is zero along all boundaries, which include the top and the free-boundary $H(r,t)$ associated with the current. Stress-free boundary conditions are imposed at the top and the free boundary. A mass flux Q with a hot temperature $\Theta=1$ is supplied at the plume neck at $r=0$. There is no velocity in the ambient surrounding. V_p is the velocity inside the plume.

$$\rho=\begin{cases}\rho_p(1-\alpha\Delta T\theta) & 0\leqslant z\leqslant H\\ \rho_s & z>H\end{cases}, \tag{1}$$

and that the fluid viscosity is given by the following simplified temperature dependent rheological law:

$$\mu(\theta)=\frac{\mu_c}{1+\Delta\mu/\mu_h\,\theta}, \tag{2}$$

where

$$\theta=\frac{T-T_c}{T_h-T_c} \tag{3}$$

is nondimensional temperature and the definitions for ρ_p, ρ_s, ΔT, T_c, T_h, α, μ_c, μ_h, and $\Delta\mu$ are given in Table I. This inverse dependence of viscosity on temperature was chosen by Bercovici[10] to facilitate an analytic derivation of the model. In this study we assume the isothermal conditions $\theta=0$ at both lower $z=H$ and upper $z=0$ boundaries of the gravity current and $0<\theta\leqslant 1$ elsewhere in the current. Also

TABLE I. Parameter description.

Parameter	Definition
g	Gravitational acceleration
H	The gravity current thickness
α	Thermal expansion coefficient of the current
κ	Thermal diffusivity of the current
c_p	Specific heat
T_c	Temperature of the surrounding media
T_h	Reference temperature hot regions of gravity current
ΔT	T_h-T_c
ρ_p	Density of the gravity current at its coldest
ρ_s	Density of the surrounding medium
$\Delta\rho_C$	$\rho_p-\rho_s$, chemical density contrast
$\Delta\rho_T$	$\rho_p\alpha\Delta T$, thermal density contrast
$\Delta\rho$	$\Delta\rho_C+\Delta\rho_T$
f	$\Delta\rho_C/\Delta\rho$, the chemical buoyancy fraction
μ_c	Dynamic viscosity at T_c
μ_h	Dynamic viscosity at T_h
$\Delta\mu$	$\mu_c-\mu_h$

we assume a self-similar temperature profile. It was shown by Bercovici and Lin[11] that parabolic profile is the dominant term in the overall vertical temperature profile, since higher order contributions typically decay away relatively rapidly because of the large thermal gradients. The assumption of $\theta=0$ at the fluid–solid interface is an oversimplification. In reality, thermal diffusion would establish a higher, radially varying temperature, that reduces the viscosity and affects the flow. In addition, the symmetry of self-similar temperature profile can be affected by viscous heating, which induces thermo-mechanical feedback. This feedback may trigger localization and self-lubrication effects for certain boundary conditions.[22] Moreover, it has been shown[23] that a temperature-dependent thermal diffusivity can cause even greater shear localization because variable diffusivity, being lower, can trap the heat locally. However, these additional effects are not considered in this modeling effort and thus the temperature profile is assumed to be

$$\theta(r,z,t)=\Theta(r,t)F_0\left(\frac{z}{H}\right), \tag{4}$$

where $\Theta=(1/H)\int_0^H\theta dz$ is the vertical average of nondimensional temperature and $F_0(\xi)=6\xi(1-\xi)$. Despite the fact that the gravity current model used in this study is rather crude, it provides us with a strong motivation for further investigation of viscous heating in gravity currents because of its potentially important impact on many environmental flow situations.

A. Model equations

The model equations are formally derived by considering conservation of mass and energy of Boussinesq fluid for a control volume in a shape of infinitesimally thin cylindrical shell of height H, radius r and thickness dr

$$\frac{\partial H}{\partial t}+\frac{1}{r}\frac{\partial}{\partial r}\left(r\int_0^H v_r dz\right)=v_z|_{z=0}-v_z|_{z=H}, \tag{5}$$

$$\frac{\partial T}{\partial t}+\frac{1}{r}\frac{\partial}{\partial r}\left(r\int_0^H v_r T dz\right)=(v_zT)|_{z=0}-(v_zT)|_{z=H}-\kappa\left.\frac{\partial T}{\partial z}\right|_{z=0}+\kappa\left.\frac{\partial T}{\partial z}\right|_{z=H}+\frac{1}{\rho_p c_p}\int_0^H\Phi dz, \tag{6}$$

where T is the temperature of the gravity current, v_r and v_z are, respectively, radial and vertical velocity components of the gravity current, c_p is the specific heat, Φ is the dissipative heat source approximated by the most dominant term in the shear flow geometry

$$\Phi=\mu\left(\frac{\partial v_r}{\partial z}\right)^2, \tag{7}$$

κ is the thermal diffusivity of the current, which is here assumed to be constant. Note since we adopted the Boussinesq approximation for the gravity current, then the fluid is considered to be incompressible except for the buoyancy

term in the vertical momentum equation and, thus, density in the continuity and energy equations is assumed to be constant.

Assuming that the vertical velocity of the material being injected into the current through one of the horizontal boundaries is $W_0(r,t)$ and that the temperature T_{in} of the injected material is T_h the model equations (5) and (6) can be rewritten as

$$\frac{\partial H}{\partial t}+\frac{1}{r}\frac{\partial}{\partial r}\left(r\int_0^H v_r dz\right)=W_0, \tag{8}$$

$$\frac{\partial H\Theta}{\partial t}+\frac{1}{r}\frac{\partial}{\partial r}\left(rH\Theta\int_0^H v_r F_0\left(\frac{z}{H}\right)dz\right)$$

$$=W_0\theta_{\text{in}}-\frac{\kappa\Theta}{H}(F_0'(0)-F_0'(1))+\frac{1}{\rho c_p\Delta T}\int_0^H\Phi dz, \tag{9}$$

where $\theta_{\text{in}}=1$ is the nondimensional temperature of the injected material. Following Bercovici and Lin[11] we assume $W_0(r,t)$ to be constant in time and defined by

$$W_0=\frac{Q_0}{\pi a^2}\exp\left(-\frac{r^2}{a^2}\right), \tag{10}$$

where $Q_0=2\pi\int_0^\infty W_0 r dr$ is the total volumetric flux into the current and a is the radius defining the flux width.

Integrating the creeping flow equations in both vertical and horizontal directions with density and viscosity respectively given by Eqs. (1) and (2) one can obtain an approximate analytical expression for the radial velocity v_r (for details see Ref. 11). Substituting this expression into Φ, integrating Eqs. (8) and (9) over the thickness of the layer, and rounding out the resulting numerical constants, as discussed in the Appendix of Ref. 11, we obtain the following dimensional model equations:

$$\frac{\partial H}{\partial t}+\frac{1}{r}\frac{\partial}{\partial r}(rq)=W_0, \tag{11}$$

$$\frac{\partial H\Theta}{\partial t}+\frac{1}{r}\frac{\partial}{\partial r}(rq\Theta)$$

$$=W_0-\frac{\kappa\Theta}{H}(F_0'(0)-F_0'(1)),$$

$$+\frac{(\Delta\rho g)^2H(1+\nu\Theta)}{4C\mu_c\rho_p c_p\Delta T}\left[\frac{\partial}{\partial r}(fH^2+(1-f)\Theta H^2)\right]^2, \tag{12}$$

with q given by

$$q\approx-\frac{\Delta\rho g H^2}{2C\mu_c}(1+\nu\Theta)\frac{\partial}{\partial r}(fH^2+(1-f)H^2\Theta), \tag{13}$$

where $\Delta\rho=\Delta\rho_C+\Delta\rho_T$, f is the chemical buoyancy fraction described in Table I, and the constants C and ν depend on the boundary conditions for v_r. In this paper we consider two types of boundary conditions:

(1) no-slip, $v_r=0$, at the upper, $z=0$, and lower, $z=H$, boundaries;
(2) no-slip at the upper boundary and free-slip, $\partial v_r/\partial z=0$, at the lower boundary.

It was shown in Bercovici[10] that these two types of boundary conditions results the following values of C and ν

$$(C,\nu)=\begin{cases}\left(3,\dfrac{9}{10}\dfrac{\Delta\mu}{\mu_c}\right) & \text{for } \left.\dfrac{\partial v_r}{\partial z}\right|_{z=H}=0\\ \left(12,\dfrac{3}{5}\dfrac{\Delta\mu}{\mu_c}\right) & \text{for } v_r|_{z=H}=0\end{cases}. \tag{14}$$

It is important to note that the choice of boundary conditions does not change the general form of Eqs. (11)–(13), instead it changes the actual value of coefficients C and ν.

B. Boundary and initial conditions

Two different types of boundary conditions are investigated:

(1) constant volume, $V=2\pi\int_0^H Hrdr=V_0$, $Q_0=0$;
(2) constant flux, $Q_0>0$.

The physical relevance of these boundary conditions is discussed in detail in Sec. III. Here we just present the mathematical formulation of these two types of boundary conditions.

Since we assumed the axial symmetry of the gravity current and the finite width of the volume flux into the gravity current, i.e., the absence of point mass of heat sources, then the only physical boundary conditions at $r=0$ that can be imposed on the gravity current are the Neumann type given by

$$\left.\frac{\partial H}{\partial r}\right|_{r=0}=0,\quad \left.\frac{\partial\Theta}{\partial r}\right|_{r=0}=0. \tag{15}$$

These boundary conditions are for both constant volume and constant flux cases. Note that boundary conditions (15) are different from the ones proposed by Bercovici and Lin,[11] where they assume Dirichlet type boundary condition $\Theta=1$ for constant flux case. These boundary conditions are inconsistent with energy equation, since for small gravity current thickness, that is observed initially for constant flux case with zero initial volume, the mean temperature can be less then unity, due to excessive heat loss at the other boundary of the gravity current. Because the model equations are hyperbolic in character, we do not need to specify boundary conditions at $r\to\infty$.

In order to be able to compare our results with the results obtained by Bercovici and Lin[11] for the case without viscous heating, we have chosen the same initial conditions as in Ref. 11:

$$H|_{t=0}=\begin{cases}\dfrac{4}{3}\dfrac{V_0}{\pi r_0^2}\left(1-\dfrac{r^2}{r_0^2}\right)^{1/3} & r\leqslant r_0\\ 0 & r>r_0\end{cases}, \tag{16}$$

$$\Theta|_{t=0}=\exp\left(-\left(\frac{r}{r_0}\right)^{20}\right), \tag{17}$$

TABLE II. Ec for different applications (ice sheets, mantle plumes, lavas, flooding currents).

	$\Delta\rho\ \left(\frac{kg}{m^3}\right)$	$c_p\ \left(\frac{kJ}{kgK}\right)$	Height (m)	ΔT (K)	Ec
Glass–Air	0.9995	0.7	10^{-1}	10^3	7.14×10^{-7}
Flood lavas–Air	0.9996	1.4	2×10^3	10^3	7.17×10^{-3}
Plume–Mantle	0.5	1.4	10^4	3×10^2	5.95×10^{-2}
Glacier–Air	0.9986	2.22	2×10^2	10	4.50×10^{-2}
Antarctic ice sheet	0.9986	2.22	2×10^3	10	4.50×10^{-1}

where r_0 is the radius of the edge of the initial current.

C. Nondimensionalization

In order to obtain nondimensional equations governing the evolution of gravity currents, we have nondimensionalized the height of gravity current H by

$$H_0=\begin{cases}\left[\dfrac{2C\mu_c Q_0}{\Delta\rho g(1+\nu)}\right]^{1/4} & Q>0\\ \left[\dfrac{2C(F_0'(0)-F_0'(1))\kappa\mu_c V_0}{\Delta\rho g(1+\nu)}\right]^{1/6} & Q=0\end{cases}, \tag{18}$$

the radial coordinate r and radius a by

$$R=\sqrt{\frac{(1+\nu)\Delta\rho g H_0^5}{2C(F_0'(0)-F_0'(1))\kappa\mu_c}}, \tag{19}$$

time t by

$$t_0=\frac{H_0^2}{(F_0'(0)-F_0'(1))\kappa}, \tag{20}$$

and flux q by

$$q_0=\frac{\Delta\rho g H_0^4(1+\nu)}{2C\mu_c R}. \tag{21}$$

With this nondimensionalization we obtain the following nondimensional model equations describing the evolution of nondimensional depth H and temperature Θ:

$$\frac{\partial H}{\partial t}=-\frac{1}{r}\frac{\partial}{\partial r}(rq)+W, \tag{22}$$

$$\frac{\partial H\Theta}{\partial t}=-\frac{1}{r}\frac{\partial}{\partial r}(rq\Theta)+W-\frac{\Theta}{H}+Ec\,\frac{1+\nu}{1+\nu\Theta}\,\frac{q^2}{H^3}, \tag{23}$$

$$q=-\frac{1+\nu\Theta}{1+\nu}H^2\frac{\partial}{\partial r}(fH^2+(1-f)\Theta H^2), \tag{24}$$

where

$$W=\frac{Q}{\pi a^2}\exp\left(-\frac{r^2}{a^2}\right), \tag{25}$$

Q is nondimensional net volume flux of fluid into the gravity current, V is nondimensional volume of fluid at $t=0$, and Ec is the Eckert number given by

$$Ec=\frac{\Delta\rho g H_0}{2\rho_p c_p\Delta T}. \tag{26}$$

We note that this particular definition of the Eckert number is not the usual one used. It is used here for consistency in order to denote the contribution arising from the viscous dissipation term. The values of Ec for different technological and geophysical situations of gravity current theory are presented in Table II.

Within the framework of the shallow-water approximation, Eqs. (22)–(24) prescribe the thermal-mechanical evolution of gravity current in the presence viscous dissipation. The strength of viscous heating is controlled by the Eckert number Ec. In the case when viscous heating is negligible, i.e., $Ec=0$, we recover the equations of Bercovici and Lin.[11] As it will be demonstrated in the subsequent sections, the effect of viscous heating can be substantial, and thus the model equations presented in this paper give a more general thermal-mechanical framework, as compared to that given in Ref. 11.

D. Numerical method

Equations (22)–(24) are solved numerically using standard second-order finite volume total variation diminishing (TVD) scheme.[24,25] To avoid the singularity for $H=0$, the thermal diffusion term Θ/H in energy equation (23) is replaced by $\Theta H/\max(H^2,H_{\min}^2)$, where $H_{\min}$ is taken to be 10^{-3}. The problem is solved for 2400 evenly distributed finite-difference points in r.

III. RESULTS

In this section we will investigate two scenarios of plume development, involving different boundary conditions of the mass conservation. Although these issues have been posed for plume dynamics, they can be readily applied to other situations as well, such as ice-sheet creep and lava flow. First, we regard an uprising plume as able to be detached from sources of hot and/or light material, e.g., Ref. 26 during its ascent from excessive buoyant forces in the head or other reasons such as choking of the plume stem. Alternatively for slow rising rates, e.g., Ref. 27 the plume head may ascend with its entire integrity, including the plume stem.

We have examined these two scenarios in two sets of numerical experiments with particular emphasis on the effects of viscous dissipation and the interaction with temperature-dependent viscosity. The first set deals with the

evolution of the plume head, subsequent to its detachment from the plume neck. The volume of the plume head is constant and its expansion is only due to buoyant forces. The second set considers the plume head as being connected to the plume neck and a constant mass flux condition is applied for this purpose. In this case the evolution of the plume head is driven by the thermal and chemical buoyant forces, the impulse from the mass injection through the plume neck and the heat produced by viscous heating.

A. Constant volume gravity currents

In this section we will investigate the influence of thermal buoyancy, temperature-dependent viscosity and viscous dissipation on the evolution of the constant volume gravity currents ($V=1$, $r_0=0.1$). This model is governed by three control variables. The first is the viscosity contrast of the temperature-dependent rheology, ν [the definition given in (14)]. This contrast represents the relative viscosity variation between the cold and hot portions of the plume. The second control variable f denotes the portion of the density variation due the compositional density contrast between the gravity current and underlying medium. These two parameters are the same as proposed by Bercovici and Lin.[11] The Eckert number Ec, which is novel in gravity current problems, measures the relative importance between shear heating and the other heat-transfer contributions. This parameter, Ec, varies between 0 (no dissipation) as in the case of Ref. 11 and a quantity of $O(1)$ (see Table II). Relatively low values of the Eckert number are found for some physical situations. Higher values of Ec can result in extremely high temperatures, which can result in partial and eventually wholesale melting. The fluid dynamics of melting and the attendant multiphase flow physics, e.g., Ref. 28 are not considered in this modeling effort.

We note that the combined effects of temperature-dependent viscosity and thermal buoyancy have been studied previously by Bercovici,[10] Bercovici and Lin,[11] Wylie and Lister,[29] but they all have neglected the potentially important role played by viscous dissipation in promoting a nonlinear feedback to the thermal regime especially at the base of the gravity current. Therefore, we have focused our efforts in drawing attention to the impact on the thermal-mechanical structure caused by viscous dissipation. In this connection Schubert *et al.*[30] and Yuen *et al.*[31] have already studied the effects of shear heating in the thermal boundary layer with a realistic olivine-rheology having a strong temperature-dependence and found that shear heating could be pronounced. But these studies dealt with steady-state boundary layers. Here we will address the issue of the temporal evolution of gravity currents with dissipation.

In Fig. 2 we show the results of gravity currents with constant viscosity. The shape of the currents reveals small differences from variations in the intensity of the dissipation, Ec varying from 0 to 0.01. The temperature profiles show a very sharp peak at the edges of the current from local dissipation. From the bottom panel of Fig. 2 we see that the production of shear heating reaches a maximum at the edges. The gravity current tends to move faster with higher values

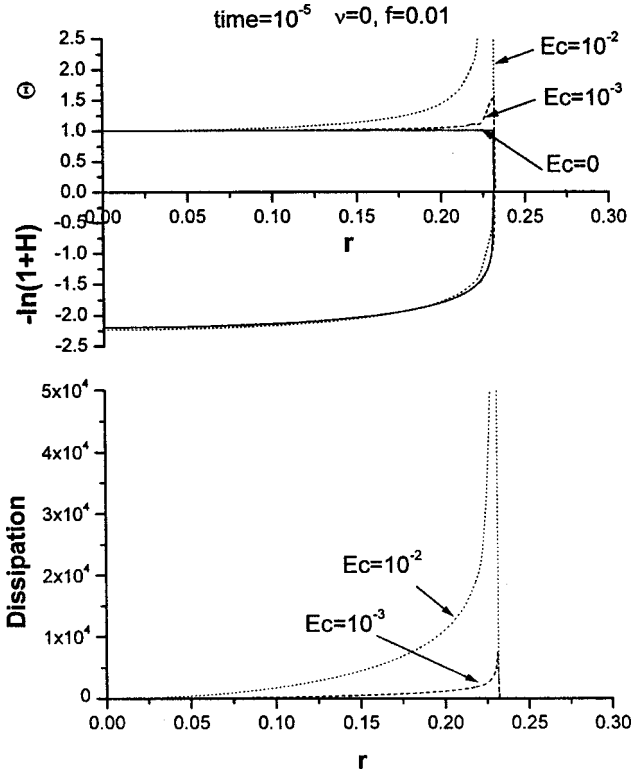

FIG. 2. The temperature Θ, the logarithm of the height H and the dimensionless rate of shear dissipation as a function of the radius. The time is taken in the incipient stage. $f=0.01$ means that it is primarily driven by thermal buoyancy. $\nu=0$ means that constant viscosity is employed. Ec is the Eckert number, measuring the strength of viscous heating. The resolution for the current consists of 2400 evenly distributed finite-difference points in r. Constant volume boundary condition is imposed.

of Ec, however, the increase from viscous heating is not that dramatic. The hot portions of the current heated by viscous heating do not affect the flow dynamics too much because of the small volume of the heated part relative to the total volume of the entire current system.

The sharp increase in the temperature at the current edge does influence the front. A less steeper front is formed with higher Ec. Thus shear heating works against temperature-dependent viscosity and thermal buoyancy, which tend to produce a steeper front in the absence of shear heating.[11] However, highly localized buoyancy anomaly is generated by the very strong lateral thermal contrast produced by shear heating at the edge.

In Fig. 3 we study the influence of temperature-dependent viscosity in gravity current with viscous dissipation. Both the magnitude of the heating and the temperature anomaly are increased in this variable viscosity gravity current. The temperature at the edge can exceed the injection temperature by a factor of 4. Such a high temperature would result in melting, which puts the flow into a different flow regime altogether. Dissipation reduces the viscosity and causes a slight increase in the expansion rates of the current. The heating causes a less steep slope of the front, thus compensating for the steepening effect found for temperature-dependent viscosity.[10,11,29]

In Fig. 4 we study a situation in which there is no ther-

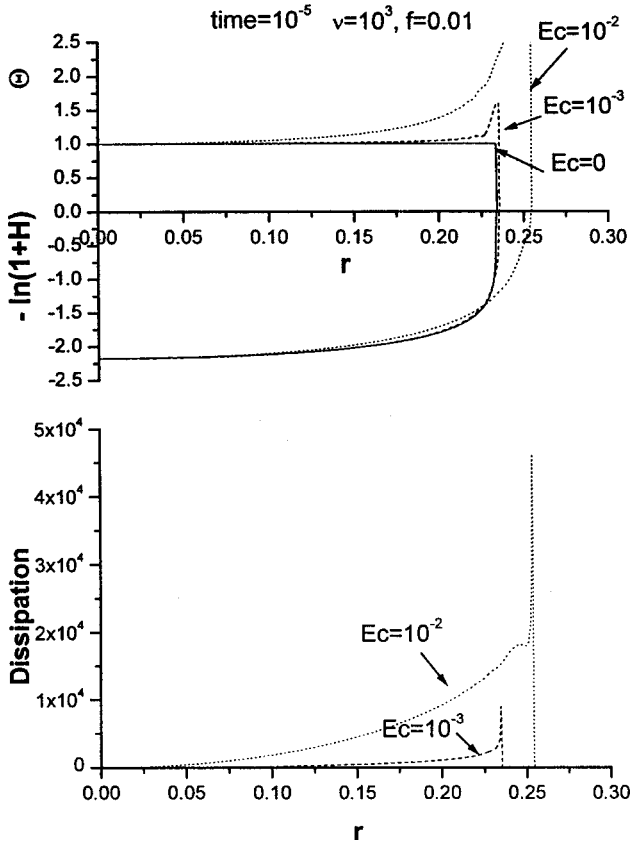

FIG. 3. Same as for Fig. 2, except for temperature-dependent viscosity with viscosity contrast $\nu=10^3$.

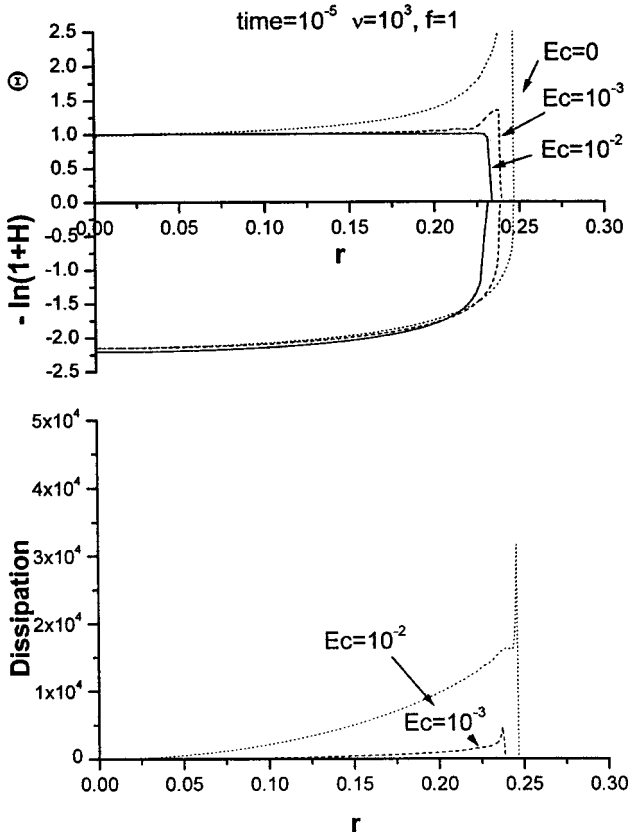

FIG. 4. The same as for Fig. 3, except now chemical buoyancy dominates with $f=1$.

mal buoyancy ($f=1$), while the viscosity contrast due to temperature ν is set to 10^3. In this situation the buoyancy comes only from the compositional differences. However, the temperature distribution inside the current can alter the viscosity and consequently the geometry and rate of expansion of the currents. As will be shown later, inclusion of viscous dissipation generally accelerates the currents. The lower panel of Fig. 4 shows that the dissipation is also focussed at the edge of the current as in the previous case (Fig. 2). This localized heating increases dramatically the temperature at the edge, while not influencing the major parts of the current elsewhere. However, the overall flow dynamics of the current is governed by the interaction between all parts of the current. Even an extremely high temperature at the edge will not greatly influence the flow, because the rest of the current still has a high viscosity, which restricts the whole flow.

In Fig. 5 we focus on the effects of an intermediate strength in thermal-chemical forcing ($f=0.5$) and temperature-dependent viscosity with $\nu=1000$. Viscous dissipation in this situation is lower than the constant viscosity case (Fig. 2) but greater than the case with only compositional buoyancy ($f=1$), shown in Fig. 4. In the incipient stages, currents with greater amounts of viscous dissipation move faster and the rate of areal expansion of the current exceeds 100% compared to the case without any dissipation, which can be clearly observed in the insert of Fig. 6. This argues for the importance of viscous dissipation in many geophysical situations (see Table II), as the maximum Eckert number displayed here is only 0.01, which is typical by geophysical standards.

Figure 6 summarizes the effects of viscous dissipation for a viscosity contrast ν of 10^3. We look at the evolution of the maximum radius reached by the current as a function of time for Ec from 0 (no dissipation) to $Ec=0.01$ (moderate dissipation). It is evident from inspection of the figure that there are three distinct stages in the evolution. The first stage occurs at very early time, when the temperature inside the gravity current is uniformly very high and, therefore, variations of viscosity and buoyant forces are small. These conditions would well correspond to the situation of an isoviscous current, described in Huppert.[21] Accordingly, at this stage the $t^{1/8}$ asymptotic relationship of Huppert[21] is well suited for describing the rate of current expansion. For the same reason, at later times after most of the heat has been released, the same $t^{1/8}$ asymptotic relationship should be found because a nearly constant ambient thermal condition is attained. Due to the cooler and lower temperatures the viscosity of the currents become higher. Thus in the log–log plot shown in Fig. 6 this portion of the evolution achieves an asymptotic state, whose slope is parallel to the incipient stage, but lying lower.

A transition between these two end-member $t^{1/8}$ asymptotic families displayed in Fig. 6 seems paradoxical. However, the slowdown during the transition stage is apparent and is attributed to the log–log representation. The actual

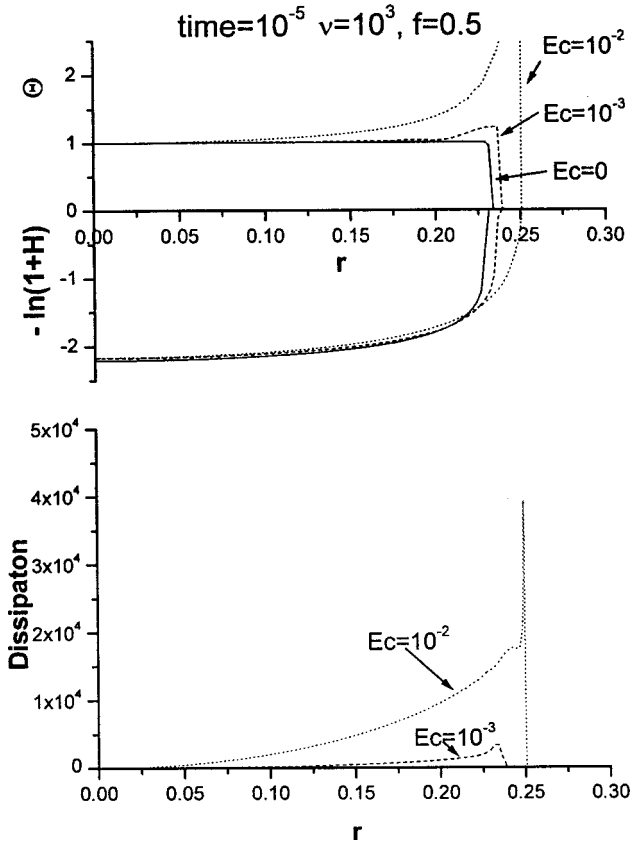

FIG. 5. The same as for Fig. 4, except now there is more thermal buoyancy $f=0.5$, such that chemical and thermal buoyancies are the same.

rate of the expansion decreases monotonically over the time. Nevertheless, the log–log plot (Fig. 6) allows us to distinguish clearly three stages corresponding to different thermomechanical regimes. The greater thermal buoyancy ($f=0.5$) also favors a longer period of transition.

We emphasize that this three-stage evolutionary process is characteristic of a fluid with a temperature-dependent viscosity and does not depend too much on viscous dissipation, which only induces a longer transition period. This three-stage behavior comes as a result of the interaction between the two quasi-isothermal regimes. The first regime corresponds to the early stage of a uniformly high temperature, whereas the third stage represents the later times when most part of the current has almost uniformly low temperature. Since both asymptotes are parallel in log–log plot, this means that the transition regime must have a smaller logarithmic rate of expansion.

Finally, it should be noted, that for constant volume gravity current, viscous dissipation is only important at the early, incipient, stage of its expansion. This can be easily explained by looking at the model equations (13) or (24). The strength of viscous dissipation is proportional to H^3, which is drastically decreases with the spreading of the gravity current. Thus, viscous dissipation only affects the initial gravity current expansion, which can be clearly seen on the insert of Fig. 6, i.e., gravity currents with higher Ec moves faster initially. Once the gravity current expands sufficiently so that viscous dissipation is negligible, the flow can be well approximated by the isoviscous solution of Huppert.[21] For this reason, we have only displayed in this section results associated with the incipient stage of the gravity current expansion.

B. Constant flux gravity currents

In this section we will consider the effects of viscous dissipation on gravity currents for the constant flux model, which has a continuous feeding of plume material ($V=0$, $Q=1$, $a=0.1$). This model corresponds to a situation, when the uprising part of the plume is connected to the bottom part with the high-temperature material, and is observed for low-

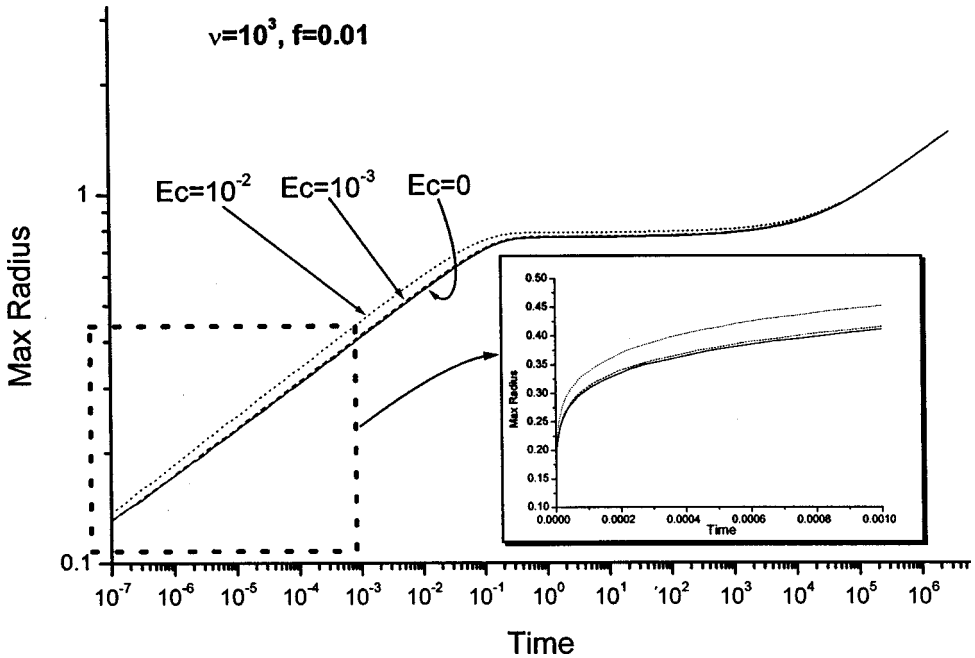

FIG. 6. The evolution of the maximum radial extent of the current with time. Viscosity is temperature-dependent with $\nu=10^3$ and the forcing is primarily thermal, f being 0.01. Inset shows the initial stages. Constant volume condition is employed.

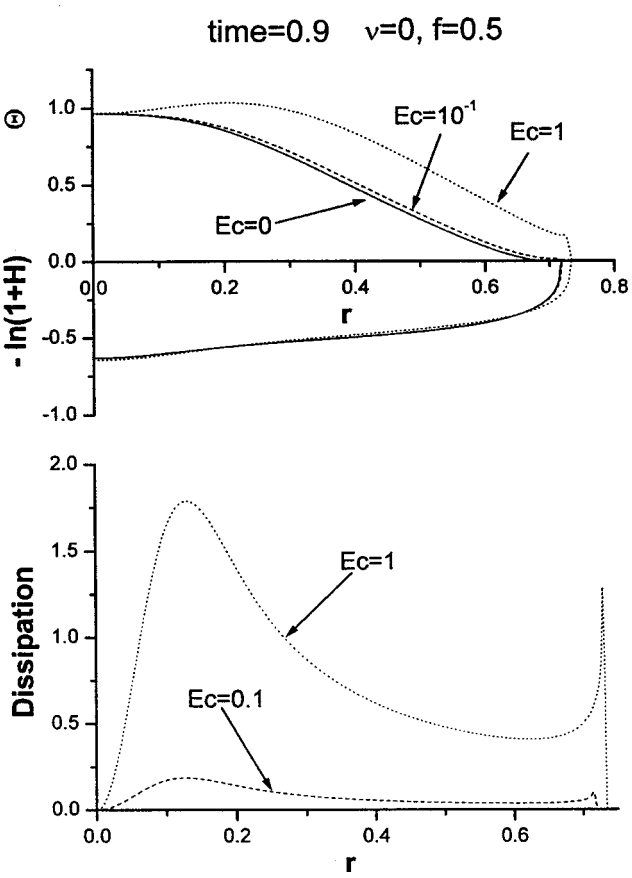

FIG. 7. The temperature, the logarithm of the height and the dimensionless shear heating as a function of the radius. The time is taken in the long time regime. Constant viscosity is used with a $f=0.5$ (equal partitioning between thermal and compositional buoyancy). A constant flux condition is imposed. Same grid is used as in the constant volume cases.

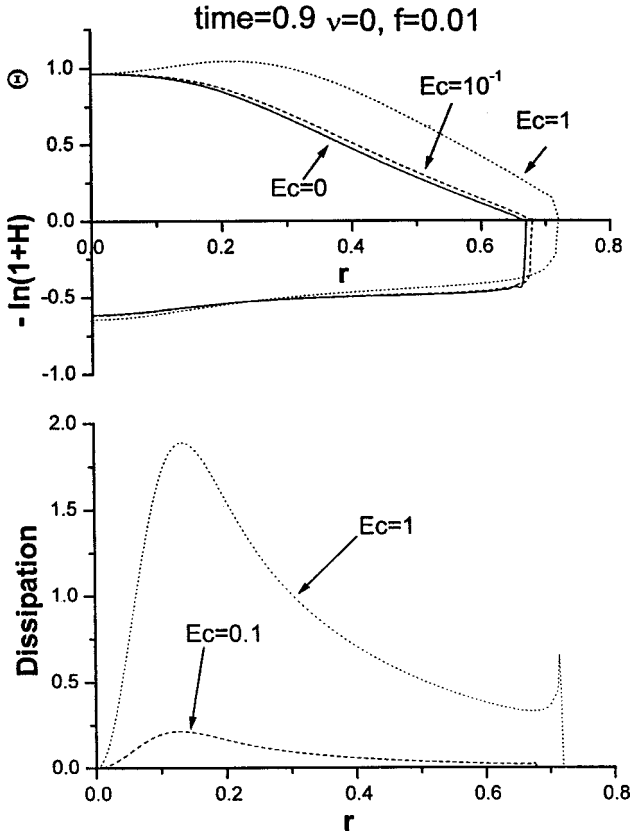

FIG. 8. Same as for Fig. 7, except a primarily thermally driven flux ($f=0.01$) is imposed.

Rayleigh number convection.[32] Even in high-Rayleigh number situation, a continuous plume can exist for depth-dependent properties in mantle rheology.[12,13,33]

The same three parameters, f, ν, and Ec are the control variables of the constant flux model. For the sake of simplicity, the mass flux is assumed to be constant in time.

In contrast to the constant volume case, which has buoyancy as the sole agent of forcing, there are two sources of forcing for the constant flux model. The first is the buoyancy, which is a volumetric source and the second comes from the impulse flux through the plume neck. The impulse flux can change radically the behavior of the gravity current.[10,11,21] This set of model is able to sustain much higher dissipation rate without melting because of the stabilizing influence due to the faster advecting cold material going from the current to its edge.

As in the case of the constant volume, higher values of Ec or dissipation produce faster running currents. This phenomenon can be observed in Fig. 7, where the current with higher Ec is able to extend further. However, this difference disappears later, when the current slows down and the strain-rate at the edge becomes too slow to maintain significant viscous dissipation and hence stops producing hot temperatures. In contrast to the constant volume model, the highest temperatures are also found in the middle portion of the current. Such a difference can be explained by the hot material being injected close to the axis of the current and second (lower panel of Fig. 7) a very high rate of dissipation is produced close to the axis. This amount of shear heating is a result of the high strain-rate in this region caused by the large radial variation in the volume flux $W(r)$. In real situation this effect is further enhanced by the sharp bending of the vertical flow to horizontal flow about a stagnation point, that produces a prodigious amount of heat, as has been shown in three-dimensional high Rayleigh number convection.[12,13]

An increase of thermal buoyancy ($f=0.01$) in Fig. 8 flattens the plateau portion of the current and makes the ''cliff'' steeper. As in the constant volume case, increase of Ec or dissipation makes the cliff less steep and facilitates faster expansion of the current.

In Fig. 9 we demonstrate the dramatic consequences of temperature-dependent viscosity in altering the spatial distribution of the shear heating and the dynamical impact on the geometrical structure of the currents. There is no thermal buoyancy in this model, as f is 1. With the constant flux condition, larger values of Ec can be tolerated, before the melting would come into the picture.

The height profiles are different in appearance from the case dominated by thermal buoyancy ($f=0.01$ in Fig. 8). Higher dissipation is again emphasized at the edges because of the temperature-dependent viscosity. However, in contrast to the constant volume situations (Fig. 4), high rates of shear

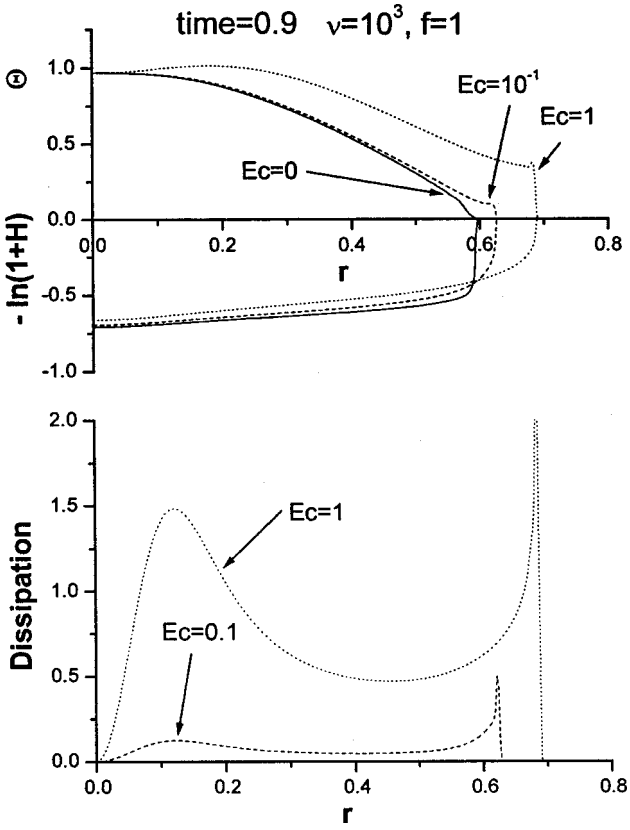

FIG. 9. Same as for Fig. 8, except a temperature-dependent viscosity with $\nu=10^3$ and a chemically dominated flux ($f=1$) is imposed.

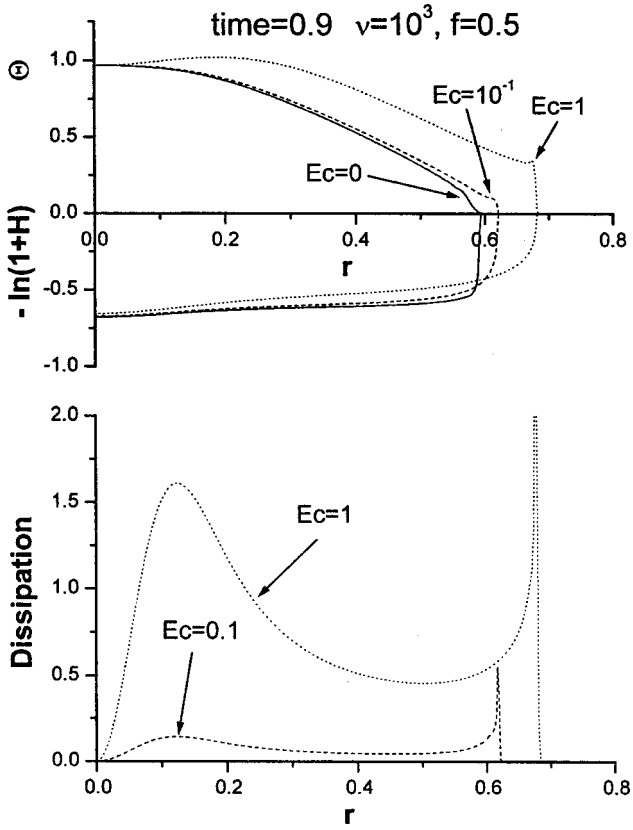

FIG. 10. Same as for Fig. 9, except an equally partitioned thermal-chemical flux ($f=0.5$) is maintained.

heating do not provoke hot temperatures because of the advection. The constant supply of relatively cool material from the central portion of the current to the edge maintains a low temperature at the edge. The maximal temperature is located at the axis of the currents for low-dissipation situations ($Ec=0.1$). For extreme cases of intense dissipation ($Ec=1$) the maximum temperature moves toward the edge. This effect is due to the stronger effect of dissipation enhanced by the impulse flux originating from the plume neck. In the lower panel of Fig. 9 we can discern readily a very high dissipation rate for $Ec=1$ takes place close to the plume neck.

Figure 10 portrays gravity currents with temperature-dependent viscosity $\nu=10^3$ and a moderate amount of thermal buoyancy ($f=0.5$). It has been suggested by Bercovici and Lin[11] that increasing thermal buoyancy would decelerate the current. The temperature inside the current decreases with time and consequently the driving force also diminishes with time. Independent of the intensity of shear heating, increasing thermal buoyancy favors the development of steeper edges. But similar to the previous case (Fig. 9), viscous heating induces a smoother edge.

With ever-increasing amount of thermal buoyancy, the shear heating is increased to such an extent that the maximum temperatures are no longer situated on the axis of the current and instead move distinctly toward the edge. We show this behavior clearer in Fig. 11, where f is set to 0.01. Now with a higher contribution from thermal buoyancy the dissipation is increased in the central portion of the current, while at the edges heating effects are attenuated. From the bottom panel of Fig. 11, it is obvious that the viscous dissipation at the edges is much lower than in the previous cases (Figs. 8 and 9) which are dominated by compositional buoyancy. Thus the nature of the buoyancy can seriously influence the viscous heating distribution. This partitioning of dissipation and dependence on f have also been found in thermal-chemical convection.[34]

Figure 12 summarizes the effect of viscous heating for the gravity currents driven by the constant flux condition. The effects of shear heating are much more pronounced in the incipient stages, where differences on the order of 10% to 20% in the maximum radius expansion can be found. This divergence in the radius caused by viscous heating continues well into the asymptotic regime, in contrast to the constant volume case (Fig. 6), where the curves merge in the second asymptotic regime. For higher heating rates ($Ec>1.0$), the divergence from the zero heating case ($Ec=0$) becomes even larger in that a different regime appears to be reached for this extreme amount of heating.

IV. DISCUSSION AND CONCLUSIONS

We have considered the effects of viscous heating on gravity currents for two different circumstances: Constant volume and constant flux conditions. The influence of temperature-dependent viscosity as well as the relative amount of thermal to chemical buoyancy, have also been examined.

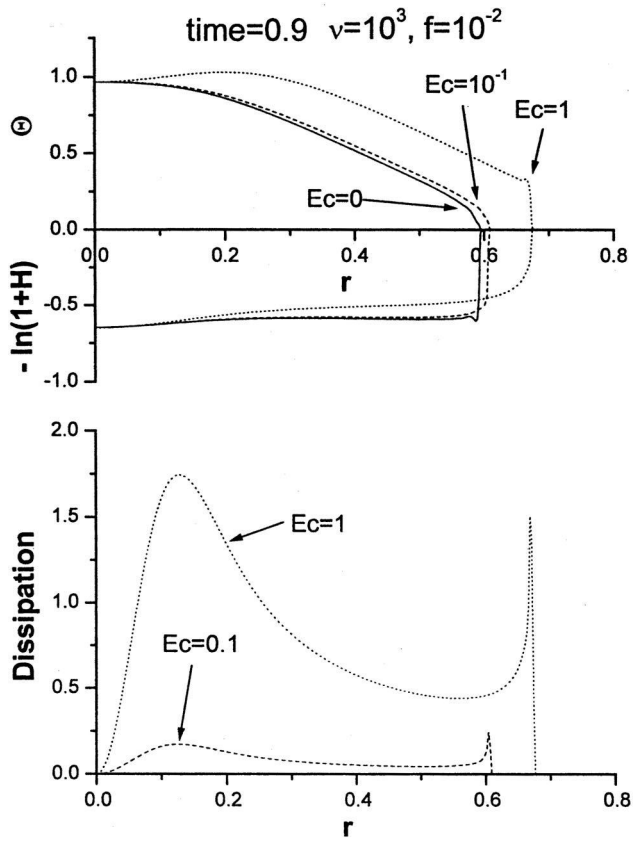

FIG. 11. Same as for Fig. 7, except now a thermally dominated flux ($f=0.01$) is maintained.

For the constant volume case a three-stage evolution was found by integrating over long times. This aspect concerning the existence of the multiple stages is new and was not found previously by Bercovici and Lin,[11] who found only two stages. The first stage follows the $t^{1/8}$ asymptotic relation for the front expansion.[21] At this stage the temperature in the current is nearly uniform. Such a condition would correspond to isoviscous flow with a negligible amount of buoyancy.

Relatively fast expansion of the stage is then followed by slow development of the current into the second stage. This stage is characterized by strongly heterogeneous temperature distribution in the current. In the third stage the current continues to slow down and it again follows the same $t^{1/8}$ asymptotic growth.

The introduction of viscous dissipation in the model results in a faster rate of expansion. Due to a high rate of strain, shear heating is localized at the edge of the constant volume currents. As a consequence of the dissipation at the early stage of gravity current expansion, hot thermal anomalies are developed at the edge, which would cause excessive buoyancy in these areas. This highly localized buoyant force may produce circular structures in the vicinity of plumes.

In contrast to constant volume case, there is only one stage of development for the constant flux gravity current. Although temperature-dependent viscosity affects the current dynamics, the rate of expansion still follows a $t^{1/2}$ asymptote which is close that predicted for a constant viscosity flow driven by constant flux.[21] As in the constant volume cases, viscous dissipation promotes a faster rate of expansion. Overheated situations associated with high Ec and small f (strong thermal buoyancy) can produce dome-shape structures on the surface of the central part of the current. In the case of surficial flows, such as lava flows and movement of large ice sheets, the outer portion of the current may become too viscous and the low viscosity part from the center portion may rise and form a secondary low viscosity flow atop the primary more viscous current. Such a situation involving viscous heating in heterogeneous media has been studied by Schott *et al.*[35] who found that intense heating is generated at the interface between the two different layers. Viscous dissipation exerts definitely a stronger influence in the constant

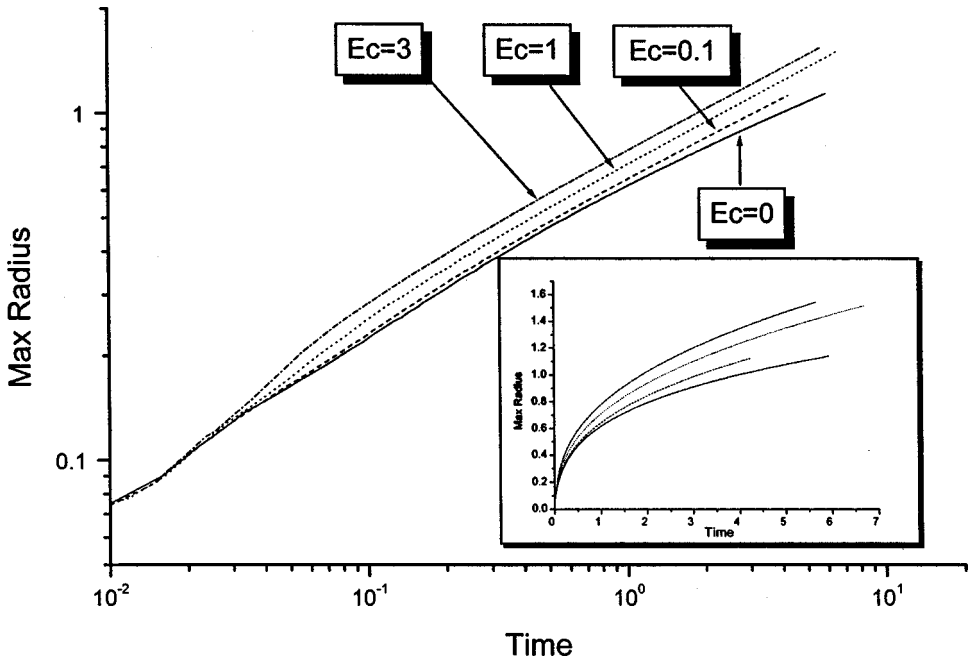

FIG. 12. Same as for Fig. 6, except a constant flux condition with ($f=0.5$) is maintained.

flux currents as compared to the constant volume currents, because of the faster velocities sustained by the flux condition.

This work should provide a strong motivation for further investigation of viscous heating in gravity currents because of its potentially important impact on many environmental flow situations. For instance, large ice-sheets in the western Antarctic have an estimated Ec close to unity, for which melting instability may be possible. Even valley glaciers can have Ec as large as 0.1. Flood basalt lavas with a thickness around 2000 meters[36,37] have values of Ec of around 0.01. The realistic boundary conditions appropriate for these environmental realistic situations probably fall between the two end-members of constant volume and constant flux. Thus there is a chance for localized instability to develop for the values of Ec quoted above. We close by noting that one can extend to more realistic geometry such as the shallow-water equation in 3D by using level-set methods[38] and wavelet decomposition[39–41] in the horizontal directions and higher order finite-difference in the vertical.

ACKNOWLEDGMENTS

We thank George Fann and Kirk E. Jordan for helpful discussion and encouragement of this problem. Support for this work was provided by the Energy Research Laboratory Technology Research Program of Energy Research of the U.S. Department of Energy under subcontract from the Pacific Northwest National Laboratory.

[1] L. Leger and J. F. Joanny, "Liquid spreading," Rep. Prog. Phys. **55**, 431 (1992).
[2] C. K. Edge, "Float glass forming: production considerations," Ceram. Bull. **6**, 936 (1992).
[3] R. Viskanta, "Review of three-dimensional modeling of glass melting," J. Non-Cryst. Solids **177**, 347 (1994).
[4] A. Ungan, "Numerical simulation of glass melting furnaces, a review," in Proceedings of the International Symposium on Glass Problems (1996).
[5] G. K. C. Clarke, "Fast glacier flow: Ice streams, surging and tidewater glaciers," J. Geophys. Res. **92,** 8835 (1987).
[6] A. J. Payne, "Limit cycles in the basal thermal regime of ice sheets," J. Geophys. Res. **100,** 4249 (1995).
[7] M. V. Stasuik, C. Jaupart, and R. S. J. Sparks, "Influence of cooling on lava flow dynamics," Geology **21**, 335 (1993).
[8] S. E. Sakimoto and M. T. Zuber, "The spreading of variable-viscosity axisymmetric radial gravity currents: applications to the emplacement of Venusian 'pancake' domes," J. Fluid Mech. **301**, 65 (1995).
[9] L. I. Lobkovsky and V. I. Kerchman, "A two-level concept of plate tectonics: applications to geodynamics," Tectonophysics **199**, 343 (1991).
[10] D. Bercovici, "A theoretical model of cooling viscous gravity currents with temperature-dependent viscosity," Geophys. Res. Lett. **21**, 1177 (1994).
[11] D. Bercovici and J. Lin, "A gravity-current model of cooling mantle plume-heads with temperature-dependent buoyancy and viscosity," J. Geophys. Res. **101,** 3291 (1996).
[12] S. Balachandar, D. A. Yuen, and D. Reuteler, "Viscous and adiabatic heating effects in three-dimensional compressible convection at infinite Prandtl number," Phys. Fluids A **5**, 2938 (1993).
[13] S. Zhang and D. A. Yuen, "Intense local toroidal motion generated by variable viscosity compressible convection in 3-D spherical-shell," Geophys. Res. Lett. **23**, 3135 (1996).
[14] S. Balachandar, D. A. Yuen, and D. Reuteler, "Localization of toroidal motion and shear heating in 3D high Rayleigh number convection with temperature-dependent viscosity," Geophys. Res. Lett. **22**, 477 (1995).
[15] S. Balachandar, D. A. Yuen, D. Reuteler, and G. Lauer, "Viscous dissipation in three dimensional convection with temperature-dependent viscosity," Science **267**, 1150 (1995).
[16] G. Schubert and D. L. Turcotte, "One-dimensional model of shallow mantle convection," J. Geophys. Res. **77**, 945 (1972).
[17] J. R. A. Pearson, "Variable viscosity flows in channels with high heat generation," J. Fluid Mech. **83**, 191 (1977).
[18] H. Ockendon, "Channel flow with temperature-dependent viscosity and internal viscous dissipation," J. Fluid Mech. **93**, 737 (1979).
[19] C. Dorsey and M. Manga, "The spreading of drops and axisymmetric gravity currents along a free surface," Phys. Fluids **10**, 3011 (1998).
[20] T. B. Larsen, D. A. Yuen, J. L. Smedsmo, and A. V. Malevsky, "Generation of fast timescale phenomena in thermo-mechanical processes," Phys. Earth Planet. Inter. **102**, 213 (1997).
[21] H. E. Huppert, "The propagation of two-dimensional and axisymmetric viscous gravity currents over a rigid horizontal surface," J. Fluid Mech. **121**, 43 (1982).
[22] V. Steinbach and D. A. Yuen, "Melting instabilities in the transition zone," Earth Planet. Sci. Lett. **127**, 67 (1994).
[23] J. Brandlund, M. C. Kameyama, D. A. Yuen, and Y. Kaneda, "Effects of temperature-dependent thermal diffusivity on shear instability in a viscoelastic zone: implications for faster ductile faulting and earthquakes in the spinel stability field," Earth Planet. Sci. Lett. **182**, 171 (2000).
[24] A. Harten, "High-resolution schemes for hyperbolic conservation-laws," J. Comput. Phys. **49**, 357 (1983).
[25] H. C. Yee, G. Klopfer, and J. L. Montagne, "High-resolution shock-capturing schemes for inviscid and viscous hypersonic flows," J. Comput. Phys. **88**, 31 (1990).
[26] P. L. Olson, "Hot spots, swells and mantle plumes," in *Magma Transport and Storage*, edited by M. P. Ryan (Wiley, New York, 1990), pp. 33–51.
[27] D. Bercovici and J. Mahoney, "Double flood basalts and plume head separation at the 660-kilometer discontinuity," Science **266**, 1367 (1994).
[28] M. Spiegelman, "Physics of melt extraction: Theory, implications and applications," Philos. Trans. R. Soc. London, Ser. A **342**, 23 (1993).
[29] J. Wylie and J. R. Lister, "Stability of straining flow with surface cooling and temperature-dependent viscosity," J. Fluid Mech. **365**, 369 (1998).
[30] G. Schubert, C. Froidevaux, and D. A. Yuen, "Oceanic lithosphere and asthenosphere: thermal and mechanical structure," J. Geophys. Res. **81**, 3525 (1976).
[31] D. A. Yuen, A. Tovish, and G. Schubert, "Shear flow beneath oceanic plates: local, nonsimilarity boundary layer solutions with olivine rheology," J. Geophys. Res., [Space Phys.] **83**, 759 (1978).
[32] A. V. Malevsky and D. A. Yuen, "Characteristics-based methods applied to infinite Prandtl number thermal convection in the hard turbulent regime," Phys. Fluids A **3**, 2105 (1991).
[33] H. P. Bunge, M. A. Richards, and J. R. Baumgardner, "Effect of depth-dependent viscosity on the platform of mantle convection," Nature (London) **379**, 436 (1996).
[34] U. Hansen and D. A. Yuen, "Formation of layered structures in double-diffusive convection as applied to the geosciences, in double-diffusive convection," in *Double-Diffusive Convection, Geophysical Monograph 94* (Amer. Geophys. Union, Washington, DC, 1995), pp. 135–149.
[35] B. Schott, D. A. Yuen, and H. Schmeling, "Viscous heating in heterogeneous media as applied to the thermal interaction between the crust and mantle," Geophys. Res. Lett. **26**, 513 (1999).
[36] A. Bjornsson, G. Johnsen, S. Sigurdsson, G. Thorbergsson, and E. Tryggvason, "Rifting of the plate boundary in North Iceland," J. Geophys. Res., [Space Phys.] **84**, 3029 (1979).
[37] C. Hofmann, G. Feraud, and V. Courtillot, "Ar 40/ Ar 39 dating of mineral separates and whole rocks from the Western Ghats lava pile: further constraints," Earth Planet. Sci. Lett. **180**, 13 (2000).
[38] J. A. Sethian, *Level Set Methods and Fast Marching Methods* (Cambridge University Press, Cambridge, 1999).
[39] O. V. Vasilyev, D. A. Yuen, and S. Paolucci, "The solution of PDEs using wavelets," Comput. Phys. **11,** 429 (1997).
[40] O. V. Vasilyev and C. Bowman, "Second generation wavelet collocation method for the solution of partial differential equations," J. Comput. Phys. **165**, 660 (2000).
[41] O. V. Vasilyev, "Solving multi-dimensional evolution problems with localized structures using second generation wavelets," Int. J. Comp. Fluid Dyn., special issue on "High-resolution Methods in Computational Fluid Dynamics" (to be published).